Lithium adsorption by $TiSe_2$ of varying concentration via density functional theory

C. Ramírez,[1] R. Adelung,[2] R. Kunz,[2] L. Kipp,[3] and W. Schattke[1,4]
[1] *Institut für Theoretische Physik und Astrophysik, Christian-Albrechts-Universität zu Kiel, Leibnizstrasse 15, D-24098 Kiel, Germany*
[2] *Technische Fakultät, Christian-Albrechts-Universität zu Kiel, Kaiserstrasse 2, 24143 Kiel, Germany*
[3] *Institut für Experimentelle und Angewandte Physik, Christian-Albrechts-Universität zu Kiel, Leibnizstrasse 19, D-24098 Kiel, Germany*
[4] *Donostia International Physics Center, Paseo Manuel de Lardizabal 4, 20018 Donostia-San Sebastian, Spain*

(Dated: Received)

Alkali adsorption on a transition metal dichalcogenide substrate has been the subject of many investigations. However, a theoretical description of its coverage dependence is still missing. In a first attempt we considered Li as an alkali prototype at a specified selection of coverages, Θ = 0.11, 0.25, 0.33, 0.5, and 1 ML, adsorbed on $TiSe_2$ (0001). By means of density-functional theory we obtained through structural optimisation the coverage dependence of the physical properties as adsorption energy, work function, and valence electron distribution. From the knowledge of the preferred adsorption sites, an optimum coverage for the most stable structure could be inferred. The work function curve shows a behaviour similar to that found for alkali adsorption on metals. The redistribution of the charge density at adsorption is presented.

PACS numbers: PACS:

I. INTRODUCTION

$TiSe_2$ belongs to a class of layered crystals based on a sandwich structure. Layers of triple planes, a transition metal atom plane sandwiched from both sides by chalcogen atom planes, are loosely bound on top of each other. These compounds are interesting because of their two-dimensional behavior which leads to a series of properties[1–4] with scientific and technical implications[5,6].

From the scientific point of view transition metal dichalcogenides (TMDCs) represent an ideal and interesting substrate for surface science studies owing to their chemically inert surfaces. For instance, it has been shown that when alkali metals are deposited on TMDCs surfaces under ultra-high vacuum conditions, they can intercalate into the bulk material or can be adsorbed on the surface of the substrate forming clusters[7,8] or networks of metallic nanowires[9,10].

Clean surfaces can be obtained via growth of single crystals by iodine gas transport reaction and subsequent UHV cleavage as well as by molecular beam epitaxy from the constituents. The structural and electronic properties of the bulk have been investigated by the standard methods and are mainly understood. The layers constitute a hexagonal structure with the c-axis parallel to the hexagonal axis and normal to the layers. The sandwiches being electronically neutral are separated by the van der Waals gap which is bridged by van der Waals forces stabilizing the structure. In fact, the valence band regime is essentially determined by chalcogen p bands (with small admixtures of metal d bands) which covalently bind within the sandwich saturating all chemical bonds. Nevertheless, the p_z orbitals perpendicular to the layer extend across the van der Waals gap and lead through their interaction to a splitting into bonding and anti-bonding states both being occupied, so that only the van der Waals forces in these compounds remain.

In contrast to the vast literature on these materials, the knowledge about the microscopic processes of growth, adsorption, intercalation etc. is rather poor[11]. In this article we present density functional theory (DFT) calculations for $TiSe_2$ with different amounts of Lithium adsorbed or intercalated. The aim is to extract the geometric structure, energetics, and electronic properties of these compounds.

The paper is organized as follows: In the next section we describe the calculational method. Sec. III concerns the changes of the geometric and electronic properties of $TiSe_2$ for different coverages of Li adsorbed on the surface, i.e., total energy, work function, and charge distribution. The changes of these properties are complemented in Secc. IV for the case of Li intercalated (within the van der Waals gap).

II. CALCULATION METHOD

The calculations performed in this study were done using the ab initio total energy and molecular dynamics program FHI98md[12]. This program evaluates the total energy of periodically repeating geometries based on density functional theory together with the local density approximation LDA for the exchange-correlation functional[13] and the pseudopotential approximation. In this case the electron-ion interaction is described by fully separable norm-conserving pseudopotentials constructed by following the scheme of Troullier and Martins[14]. These were generated using the code developed by Fuchs and Scheffler[15]. For computational efficiency the pseudopotentials are transformed into the separable Kleinman-Bylander form[16], with the s, p and d pseudopotential chosen as the local components for Ti, Se, and Li, respectively to avoid the appearance of ghost states. To ensure better transferability of the alkali pseudopotential the nonlinear form of the core-valence exchange-correlation functional is taken into account[17]. Periodic boundary conditions are used, with the eigenfunctions of the Kohn-Sham operator expanded over a plane wave basis set using an energy cutoff of 40 Ry. Two special **k**-points are used in the surface irreducible Brillouin zone (IBZ) for the Brillouin-zone integration.[18] Convergence tests performed for a higher number of **k**-points did not show any significant variation of the calculated energies. In order to improve the quality of the integration in the **k** space a Fermi-surface smearing of 0.1 eV is used and the resulting total energies are extrapolated to zero temperature. Geometries are optimized by damped Newton dynamics.

The surface is simulated by repeated slabs separated in the z direction by a vacuum region. For the adsorption structures on $TiSe_2$ (0001), three layers of $TiSe_2$ are used to model the surface with a vacuum region of 8.3 Å. To avoid any artificial adsorbate-adsorbate interaction through the slab the alkali metal is adsorbed on one side only. The resulting induced dipole moment is taken into account by applying a dipole correction[19]. The position of the atoms in the two topmost $TiSe_2$ layers and all of the adsorbed atoms are optimized by requiring that the forces on all unconstrained atoms converge to less than 0.015 eV/Å. The bottom layer was kept fixed at the bulk-like positions. Calculations with 4 layers of $TiSe_2$ and a cut-off of 60 Ry show that the adsorption energy *differences* are accurately given, which means that they change by less than 0.03 eV. The third layer, being fixed in the present calculations, showed a deviation of less than 0.05 Å when allowing it to relax in a four layer calculation. There is no significant change beyond the computational accuracy for the first two layers.

The supercells used to model Li adsorbed on the surface and Li intercalated must have the same lattice constants to make the results comparable. We chose to use the theoretical lattice constants of bulk $TiSe_2$ fully intercalated, $a_0 = 3.50$, $c_0 = 6.30$ Å [11]. We note that the calculated lattice constants are 2.7 and 2.5% smaller than the measured ones ($a = 3.60$ and $c = 6.46$ Å)[20], which is partially due to the LDA used in the calculations.

Recently, the question of accuracy of LDA/GGA (generalized gradient approximation) [21] has been discussed in view of the long-range van der Waals interaction. We are not in the position to quantitatively estimate the influence of such interactions in the DFT functional on our results, which are obtained with conventional LDA. In the past, a lot of experimental results have been confirmed with this method [22,23]. Furthermore, the specific binding of single atoms to the layered substrate obtained in this paper supports in this first access the procedure used.

In order to determine the effects of alkali adsorption on the $TiSe_2$ (0001) surface structure, the bare surface is first investigated. Calculations for the atomic relaxation of the clean surface using (3×3), $(\sqrt{3} \times \sqrt{3})$, and (2×2) periodicities were performed. These calculations provide also a test of the surface relaxation with cell size. It was found that all the interlayer distances were within 1 % independent of the supercell used.

Lithium on the surface and van der Waals adsorption sites for coverages ranging from 1/9 to a full monolayer (ML) were then studied. In particular, coverages of 0.11, 0.33 ML were calculated using (3×3) and $(\sqrt{3} \times \sqrt{3})R30^\circ$ surface unit cells respectively, while for coverages of 0.25, 0.5 and 1 ML a (2×2) unit cell was used, (see Figure V).

The coverage $\Theta = 1$ is defined as the ratio of the number of adsorbate atoms to the total number of hcp sites in the substrate. The hcp sites were found to be the energetically most stable sites for Li adsorption on $TiSe_2$ [11]. Thus, all our present calculations are referred to Li adsorbed on these sites. The adsorption energy per adatom is defined as:

$$E_{\mathrm{ad}}^{\mathrm{Li/TiSe_2\,(0001)}} = -\frac{1}{N_{Li}}[E^{\mathrm{Li/TiSe_2\,(0001)}} - (E^{\mathrm{TiSe_2\,(0001)}} + N_{Li}E^{\mathrm{Li\,atom}})], \tag{1}$$

where N_{Li} is the number of Li atoms in the surface unit cell, and the total energy of the adsorbate-substrate system, the clean $TiSe_2$ (0001) substrate, and the free Li atom, are represented by $E^{\mathrm{Li/TiSe_2\,(0001)}}$, $E^{\mathrm{TiSe_2\,(0001)}}$, and $E^{\mathrm{Li\,atom}}$, respectively.

The total energy of isolated, free atomic Li needed as a reference to determine the adsorption energy (see Eq. (1)) is calculated in a cubic cell of side length 25 a_B with the **k** point (0.5, 0.5, 0.5) for the Brillouin Zone sampling. The spin polarization effects were not included.

III. Li ADSORPTION ON $TiSe_2$ (0001)

A. Surface atomic geometry

Surface atomic geometry and work function are two of the physical quantities which change upon alkali metal adsorption. To learn about the coverage dependence of the surface atomic arrangements and related properties, calculations at five different Li coverages on $TiSe_2$ (0001) were performed. The various structural parameters obtained comprise among others the distance between the adatom and the surface, the bond length Se-Li, the inter- and intra-layer spacings, the lateral and vertical displacements of the adatom and substrate atoms, and the van der Waals gap width.

In the upper block of Table V, the optimized inter- and intra-layer distances of the substrate are resumed, while in the bottom block are listed the shifts of atomic planes relativ to pure $TiSe_2$, see Figure V. The distance d_0 from the Li adatoms to the surface roughly decreases when increasing the coverage from 0.11 to 0.5 ML. At higher coverage (1.0 ML) the distance increases again. The first interlayer spacing d_{11} increases by $\approx$ 3-7 % as a result of an inward displacement of the Ti atomic plane, see Table V (bottom). Whereas the second interatomic spacing d_{12} decreases by $\approx$ 2-5 % with respect to the pure surface. The van der Waals width, D_1, decreases for all coverages by about 2-7 % with respect to the pure surface system. Note that the calculated bulk gap of $TiSe_2$ is D_{bulk} = 3.14 Å[11]. For all coverages the second $TiSe_2$ layer keeps the relaxed position of the pure structure, see d_{21} and d_{22}. For the structures with a Li-coverage of Θ = 0.25, 0.5, and 1.0 ML, the three atomic planes of the second $TiSe_2$ layer shift inwards by the same amount; thus, no changes in the intralayer spacings with respect to the clean surface are obtained, but a reduction in the interlayer spacing D_2 of about 4%. For the other coverages there is no significant change of the interlayer spacing.

In the coverage range from 0.11 to 0.5 ML the three Se atoms in the first atomic plane coordinated to the Li adatom move radially away from it. The calculated amplitudes of these in-plane displacements are $\approx$ 0.02 Å. Small bucklings towards bulk are obtained for these three Se atoms of $\approx$ 0.02 Å for coverages less than 1 ML. As expected from the symmetry of the unit cell, no buckling is obtained for the full coverage. The Ti atom localized in the second plane, directly below the adsorbed Li, moves inwards, i.e., to the bulk, with respect to the rest of Ti atoms in the same atomic plane. This displacement increases for lower coverages, see Δd in Table V.

The table also reveals the rather exceptional case of Θ = 0.33 ML coverage yielding a substrate structure which is closest to the uncovered system. The peculiarity of this coverage is shown in other observables too.

Altogether, a compression of the whole slab can be stated when Li is adsorbed. This is explained by the charge transfer from Li to the slab and the resulting induced dipole forces contracting the substrate as a whole. Because of the different charge distributions with varying coverage a monotonous behavior cannot be expected.

B. Work function and adsorption energy

The work function, Φ, of a crystal surface is defined as the energy required to extract an electron at the Fermi level from the bulk region of a crystal to the vacuum at infinity. The calculated average work function of the clean $TiSe_2$ (0001) surface for the different supercells used is Φ=5.4 $\pm$ 0.1 eV, in agreement with experiment (5.3 eV)[24]. Figure V(a) shows the calculated work function change $\Delta\Phi$ as a function of Li coverage. This curve has the characteristic shape found for systems of alkali metal adsorbed on metallic surfaces [25,26]. Initially, it shows a rapid lowering of Φ, to a minimum ($\Delta\Phi_{min}$= -3.2 eV) at Θ = 0.5 ML, and subsequently an increase towards Θ = 1.0 ML ($\Delta\Phi$= -2.8 eV). Such a decrease in the work function upon lithium adsorption reflects the electropositive nature of Li that results in an induced dipole moment $\mu(\Theta)$.

The final increase of Φ has been attributed to a metallization of the alkali overlayer[27,28]. Taking Φ= 5.4 eV as the value of clean $TiSe_2$ (0001), we obtain a work function of 2.6 eV at 1 ML. At this coverage the saturation level has not yet been reached, since the experimental work function for Li bulk is Φ=2.93 eV [29]. That also means that a metallic behavior of the adsorbed Li system occurs at higher coverages than one monolayer. It is worth noting that such a shape of the work function change curve is obtained for other systems, e.g. Li/Mo(112)[34].

In Figure V(b) the adsorption energy of Li (hcp site) as a function of coverage is presented. The adsorption energy decreases when increasing the Li coverage from 0.11 to 0.25 ML, which indicates a repulsion between adatoms. With increasing coverage the adsorption energy reaches a local maximum at Θ= 0.33 ML, and it decreases again at higher coverages. From 0.5 to 1 ML the adatoms have to occupy next neighbor sites separated from each other by a distance of 3.50 Å, which approaches the Li-bulk lattice constant (3.40 Å)[30]. This gives rise to a strong repulsion between adatoms, which is reflected in the decrease of the adsorption energy. A complete energy landscape for Li diffusion on the surface is found in ref.[11] for Θ= 0.33 ML.

Figure V(a) shows how the adsorbate-induced dipole moment μ changes with increasing coverage. The coverage dependence of the induced dipole per adatom can be seen as a consequence of the dipole-dipole interaction, which gives rise to a depolarization with decreasing Li-Li distance.

As a rough estimate of the charge at the Li atom (with $\Theta = 0.33$, 0.5 and 1 ML), we calculated the dynamic charge. This quantity is of interest to discuss how the bond between the adsorbed alkali metal atom and the surface is best described, whether the adsorbate should be regarded as partly ionic due to a charge transfer to the substrate or as essentially neutral but strongly polarized. The dynamic charge is given by the slope of the curve when plotting the surface dipole moment versus vertical distance of Li to the surface [31]. A linear dependence of the dipole moment was obtained for the three coverages studied (for small variations of the adsorbate height), indicating an ionic bonding between Li adatoms and the substrate. At $\Theta = 0.33$ and 0.5 ML the dynamic charge values are 0.4 and 0.2 electron, whereas at $\Theta = 1.0$ ML the value is -0.3 electron. The decrease and change in sign indicates a change of the charge flow from the adatoms to the substrate at low coverage and from the substrate to the adatoms at full coverage. This can be explained as follows: according to the Langmuir-Gurney model [32,33], in a first adsorption phase the low ionisation potential of alkali metals induces a charge transfer when adsorbed on more electronegative substrates. Each partially positively charged adatom then builds up a dipole with the substrate, pointing from the negatively charged substrate to the adatom. This dipole orientation facilitates the escaping of the electrons to the vacuum, i.e. the work function of the clean substrate will strongly decrease, see Figure V(a). The electrostatic repulsion between the charged alkali ions increases with the coverage. Thus, in a second adsorption phase charge from the substrate feeds back to the alkali metal to weaken the repulsion between alkali ions, inducing an increase of the work function. At higher coverages the work function reaches a saturation level with the value of the bulk alkali metal.

A change of the ionic character of the bond is also reflected in the Langmuir-Gurney model as a change in the bond length of the alkali as the coverage is increased. This is depicted in Figure V(b), where the bond length Li-Se decreases as the coverage is increased from 0.11 to 0.5 ML, and from this coverage to a saturated overlayer it increases.

C. Charge redistribution

To analyze the nature of bonding, it is helpful to consider the *difference electron density* $n^{\Delta}(\mathbf{r})$,

$$n^{\Delta}(\mathbf{r}) = n(\mathbf{r}) - n^{0}(\mathbf{r}) - n^{Li}(\mathbf{r}), \tag{2}$$

where $n(\mathbf{r})$ is the total valence electron density of the substrate-adsorbate system, and $n^{0}(\mathbf{r})$ and $n^{Li}(\mathbf{r})$ are the electron densities of the clean substrate and the free lithium atom, respectively. The atomic geometry of the substrate is chosen from that of the relaxed adsorbate system determining its electron density by a separate selfconsistent calculation with the frozen structure. The *difference electron density* shows the depletion or accumulation of the charge density in the system owing to adatom adsorption at the surface.

For lower coverages of Li on the surface ($\Theta = 0.11$), most of the charge difference is located between the Li and the Se atoms that are next to it. Since the Li adatom is adsorbed on the hcp site, the $3d$ orbitals of the Ti atoms located immediately below this site point towards the Li position. When the amount of Li increases to $\Theta = 0.5$ the Ti $3d$ orbitals of the atoms below the adsorption sites seem to be a mixture of d_{z^2}, d_{xz} and d_{yz} with prominence of the first one, whereas for the rest of Ti atoms the d_{xz} and d_{yz} are more important. In Figure V the charge density differences, $n^{\Delta}(\mathbf{r})$, of Li adsorbed on $TiSe_2$ (0001), ($\Theta = 0.5$, and 1.0 ML) are shown. For $\Theta = 0.5$ most of the charge transfer becomes localized between Li and the Se atoms and the Li adatom is adsorbed closer to the surface than for $\Theta = 0.11$; thus, more charge is localized in Ti $3d$ orbitals, which in the bulk $TiSe_2$ case are only partially occupied. For $\Theta = 1.0$ the charge clouds between the adsorbate and the Se atoms as well as in the $3d$ orbitals of the Ti atoms are obtained, see Figure V. At this coverage there is a Li adsorbed above every Ti. This results in an enhanced occupancy of all the $3d$ orbitals of the Ti atoms, in contrasts to empty orbitals for $\Theta = 0.5$.

In Figure 6 the partial density of states (PDOS) is displayed for the constituents of the compound. The energy region between -10 eV and -20 eV shows a triple structure in the regime of the atomic Se s orbitals. These peaks originate from a crystal field splitting according to the adsorbate environment of the Se atoms which depends on coverage. The 1/3-coverage finds each upper Se atom coordinated by one occupied and two empty adsorption hcp sites. This leads to one single major unsplitted peak from the Se s orbital influenced by the neighboring Li atom. The 1/2-coverage has one upper Se atom coordinated by one occupied Li site and two upper Se both coordinated by two occupied hcp adsorption sites, i.e. one singly coordinated and two doubly coordinated Se atoms, the former leading to a peak roughly at the same position as in the 1/3 case, the latter splitting off two peaks at lower energy which coincide with the respective ones of the 1ML case. The 1 ML coverage encounters every hcp adsorption site occupied, i.e. every upper Se is coordinated by three Li atoms and shows a triple peak of s character around this energy as it should according to the three representations of C_{3v}. For smaller coverage a broad Se s band is found because of the number of coordinations present. Correspondingly, some part of the Se s charge resides on the Li atom as is confirmed by Figure 6. The unoccupied Ti d orbital shows its fingerprint also in the Li PDOS for high coverage suggesting an interaction reaching as far as that from Li to Ti which was also seen in the charge density plots above. As expected, the Se p bands with admixtures of Ti d states are present at the Li position.

IV. Li INTERCALATED

A. Diffusion in the van der Waals gap

The energetics and structural changes of Li_xTiSe_2, ($0.11 \leq x \leq 1.0$), where Li_xTiSe_2 refers to $TiSe_2$ intercalated with Li, are calculated by means of total energy calculations. Among others, the most stable positions of Li in the van der Waals gap and the energy barriers for diffusion therein are determined .

Pure $TiSe_2$ crystallizes with the 1T-CdI_2 structure, where the metal is octahedrally coordinated by the chalcogen atoms and the layers are stacked without lateral displacements. When intercalation occurs, the intercalant Li enters the van der Waals gaps between the layers. In Figure V the three interstitial sites available in the van der Waals gap are shown: one octahedral, which is surrounded by six chalcogen atoms, and two tetrahedrals, which lie in the projections below and above the chalcogen atoms (T_1 and T_2 respectively, Figure V)

The total energies of Li_xTiSe_2, (x=0.33), with Li occupying the different interstitial sites are calculated using a $(\sqrt{3} \times \sqrt{3})$ supercell (with 3 sandwiches of $TiSe_2$ and a vacuum space of $\approx$ 8 Å), with Li occupying the different interstitial sites. It was found that the octahedral site is energetically more favorable than both tetrahedral, the latter ones having equal energy, (3.58 for octahedral and 3.22 eV for tetrahedral). The corresponding binding energies for all interstitial sites are markedly higher than the ones in the surface. This reflects the fact that the interlayer sites are considerably more favorable. Furthermore, it demonstrates the strong tendency of $TiSe_2$ towards intercalation and the stability of the intercalated compound.

The migration of Li along the van der Waals gap can be described as a hopping between the different sites, i.e. octahedral → bridge → tetrahedral → bridge. The most favorable diffusion pathway from octahedral to octahedral site involves the intermediate occupation of a tetrahedral site. Both sites are separated by a saddle point (bridge site) with a binding energy of 3.15 eV. The energy difference between the octahedral and bridge site gives a diffusion barrier value of 0.43 eV. When the Li atom diffuses from a octahedral to a bridge site at Θ=0.33, d_zLiSe(3 and 4) in Table V and Figure V, it relaxes from the middle of the van der Waals gap to a position closer to the lower layer. From the bridge to a T_1 tetrahedral site the Li relaxes closer to the bottom layer, while for a T_2 it relaxes towards the top layer by the same amount [11].

For comparison, we determined also the diffusion barrier for Li in the van der Waals gap but with a bulk calculation, i.e., using a (1×1) $TiSe_2$ cell with a_0=3.50 Å and c_0=6.30 Å as lattice constants[11]. The total energy was calculated for different configurations, where the Li atom was fixed at equidistant points of the unit cell, and was allowed to relax only in the z-direction. The grid spacing was 1/4 the distance between tetrahedral and octahedral sites. Figure V shows the energy surface obtained. The diffusion path is similar to that obtained with the supercell model, but the activation barrier increases to 0.6 eV.

The diffusion barrier along the van der Waals gap is in the $(\sqrt{3} \times \sqrt{3})$ supercell model two times higher than for surface diffusion. Therefore, if the intercalating atoms enter the solid from the side, the filling of the edges is faster than the propagation of the diffusion front into the solid, which leads to a bottleneck at the edges. In previous results[11] a barrier of 3.81 eV for direct intercalation starting from the surface and penetrating perpendicularly into the van der Waals gap was found. The high value of the barrier suggests that the most probable path of intercalation is through the edges or defects of the crystal. However, even in this scenario the bottleneck seems to suppress bulk intercalation, supporting the observed enhancement by grinding the material.[36]

B. Structure vs. Li concentration

The intercalation of Li in TMDC's has been considered to be topotactic, i.e., the host structure undergoes no symmetry distortion by insertion of alkali[37]. Apart from a slight expansion of the c-axis, no change within the slabs is expected. For the study of the effects of alkali intercalation in TMDC's, several bandstructure calculations have been carried out in the past [22,38,39]. In these calculations, structure optimization was absent and experimental lattice constants had been chosen to describe the intercalated compounds. The internal structure parameter z, which determines the distances between atomic planes had been fixed to the value of the pure bulk structure. Thus, there is a lack of information about the geometric structure changes of alkali intercalated TMDC's in the near-surface region.

The most stable position for the Li atoms are the octahedral sites of the van der Waals region for all values of x.[40] The lithium intercalation complexes of $TiSe_2$ (written as Li_xTiSe_2) retain the basic structure of the original $TiSe_2$ lattice. The geometric structure of Li_xTiSe_2 is explained in Figure V. This Figure is related to Table V, in which the changes of the structural parameters are summarized. As expected, the largest change produced by intercalation is found in the expansion of the c-lattice with respect to the pure structure. The thickness of the sandwich is not significantly altered with insertion of Li_x (for any x) in agreement with [41], but the van der Waals gap width is changed relative to the clean system.

Those Se atoms that form bonds with Li atoms, and further, those Ti atoms that lie above and below these intercalated atoms, slightly shift away from them in z direction with an unaltered z position of the other atoms in the same plane. These local distortions obtained around the intercalated alkali (octahedral sites) are isolated at low x, but overlap for $x>0.25$ resulting in flat host layers. As in TiS_2, which according to Fischer *et al.*[42] revealed an overlapping distortion by Li intercalation at a lower value of x (x=0.5) than in graphite (x=0.7), here again $TiSe_2$ layers are stiffer than graphite.

C. Adsorption energy, work function, and charge density

We found that the adsorption energy decreases with increasing x with a local maximum at $x = 0.33$, see Figure V. The global dependence on concentration seems to reflect an electrostatic repulsion of the Li ions even at highest dilution when a screening could be suggested. Hibma[43] showed that the repulsion between intercalated alkali atoms is significant only within one lattice constant. From our results we have to infer that the complete ionization of the outer Li shell is hard to be fully screened on short range, instead the mutual Li repulsion diminishes the tendency to incorporate additional adsorbate. This leads to a decrease of the adsorption energy which is detected here as an overall behavior. The local maximum at $x = 0.33$ indicates a more stable configuration for this concentration. An ordered ($\sqrt{3} \times \sqrt{3}$) superstructure has been observed experimentally for Li_xTiS_2 [43], which agrees with the present calculations showing the energetically most stable structure at x=0.33. From the trend of the energy to decrease, the formation of Li islands or clusters is excluded. In UHV intercalation only limited concentrations below x=0.5 of intercalated alkali have been reported[24,44–48]. This has been attributed to the existence of a diffusion barrier for the alkali ions[48].

In Figure V the change in work function versus x is shown. We obtained that the work function decreases smoothly and no minima are observed. This trend is also observed experimentally for similar materials [7,24,49–51]. In Figure V the plot of the difference of charge density $n^{\Delta}(\mathbf{r})$ shows a symmetrical distribution in both layers separated by the van der Waals gap containing the Li atom. There is a charge transfer to the Ti orbitals though the maximum charge density is between Se atoms and Li. Charge transfer to the chalcogen was also found by Umrigar, *et al.*[38] in their FLAPW calculations on $LiTiS_2$.

V. SUMMARY AND CONCLUSIONS

The binding energies of Li atoms on the surface and in the van der Waals gap display similar behavior, but differ in absolute value by roughly 0.5 eV in favour of the intercalated structure over all Li concentrations. According to these results the most stable structure is obtained when Li occupies the hcp site on the surface and the octahedral site in the van der Waals gap. At a concentration of x=0.33 an ordered two-dimensional $\sqrt{3} \times \sqrt{3}$ superstructure is formed in both cases, in the surface adsorption plane and in the subsurface layer intercalation plane, respectively. For the bulk crystal this would lead to a three-dimensional phase transition by fixing also the period along the c direction.

For both surface and van der Waals alkali adsorption, we found a charge transfer from the alkali to the substrate. Thus, the charge transfer takes place already on the surface and can not be the driving force for intercalation as it is often assumed [52]. In contrast, an energy barrier of 3.81 eV for intercalation starting from the surface was found.[11] The charge is located between Li and Se atoms as well as in the d orbitals of Ti.

The covalent Ti-Se bond is weakened by adsorption and intercalation of Li, since for both cases a small elongation of the Se-Ti bond length is obtained.

When Li_x ($0.11 \leq x \leq 1.0$) is adsorbed on the surface the c-lattice constant decreases by about 0.05-0.21 Å, which yields a decrease in the van der Waals gap width. On the contrary, when Li is placed in the van der Waals gap, the c-lattice constant is expanded for larger concentrations.

When Li atoms are adsorbed on the surface, the changes of the work function can be well described by the Langmuir-Gurney model: at low coverages Φ decreases until it reaches a minimum around $\Theta = 0.5$ ML, and then increases approaching the value of the bulk alkali metal. On intercalating substrates the work function has a smooth decrease and no minima are observed.

ACKNOWLEDGMENTS

The support by the Deutsche Forschungsgemeinschaft through the Forschergruppe FOR 353 is gratefully acknowledged. The authors thank John von Neumann - Institut für Computing (NIC) and Rechenzentrum Kiel for providing the computing facilities.

REFERENCES

[1] J.-M. Tarascon and M. Armand, Nature **414**, 359 (2001).

[2] K. Motizuki and N. Suzuki, in *Structural Phase Transitions of Layered Transition Metal Compounds*, edited by K. Motizuki (Reidel, Dordrecht, 1986).

[3] J.A. Wilson and A.D. Yoffe, Adv. Phys. **18** 193 (1969).

[4] J.A. Wilson, F. Di Salvo, and S. Mahajan, Adv. Phys. **24**, 117 (1975).

[5] *Photoelectrochemistry and Photovoltaics of Layered Semiconductors, Physics and Chemistry of Materials with Low-Dimensional Structures*, edited by A. Aruchamy (Kluwer Academic Publisher, Dordrecht / The Netherlands, 1992).

[6] H.J. Lewerenz and H. Jungblut, *Photovoltaik* (Springer Verlag, Berlin, 1995).

[7] S. Kennou, S. Ladas, and C. A. Papageorgopoulos, Surf. Sci. **152-153** , 1213 (1985).

[8] C. Papageorgopoulos, M. Kamaratos, A. Papageorgopoulos, A. Schellenberger, E. Holub-Krappe, C. Pettenkofer, and W. Jaegermann, Surf. Sci. **275**, 314 (1992).

[9] R. Adelung, L. Kipp, J. Brandt, L. Tarcak, M. Traving, C. Kreis, and M. Skibowski
Nanowire networks on perfectly flat surfaces
Appl. Phys. Lett. **74**, 3053 (1999).

[10] R. Adelung, J. Brandt, K. Roßnagel, O. Seifarth, L. Kipp, M. Skibowski, C. Ramírez, T. Strasser, and W. Schattke, Phys. Rev. Lett. **86**, 1303 (2001).

[11] C. Ramírez and W. Schattke, Surf. Sci. **482-485**, 424 (2001).

[12] M. Bockstedte, A. Kley, J. Neugebauer, and M. Scheffler, Comp. Phys. Comm. **107**, 187 (1997).

[13] D. M. Ceperley and B. J. Alder, Phys. Rev. Lett. **45**, 566 (1980).

[14] N. Troullier and J. L. Martins, Phys. Rev. B **43**, 1993 (1991).

[15] M. Fuchs, M. Scheffler, Comput. Phys. Commun. **116**, 1 (1999).

[16] L. Kleinman and D.M. Bylander, Phys. Rev. Lett. **48**, 1425 (1982).

[17] S.G. Louie, S. Froyen, and M.L. Cohen, Phys. Rev. B **26**, 1738 (1982).

[18] S. L. Cunningham, Phys. Rev. B **10**, 4988 (1974).

[19] J. Neugebauer and M. Scheffler, Phys. Rev B **46**, 16067 (1992).

[20] M. S. Whittinghan and F. R. Gamble, Mater. Res. Bull. **10**, 363 (1975).

[21] H. Rydberg, M. Dion, N. Jacobson, E. Schröder, P. Hyldgaard, S.I. Simak, D.C. Langreth, and B.I. Lundqvist, Phys. Rev. Lett. **91**, 124602-1 (2003).

[22] P. Blaha, J. Phys.: Condens. Matter **3**, 9381 (1991).

[23] D.R. Allan, A.A. Kelsey, S.J. Clark, R.J. Angel, and G.J. Ackland Phys. Rev. B **57**, 5106 (1998).

[24] W. Jaegermann, C. Pettenkofer, A. Schellenberger, C.A. Papageorgopoulos, M. Kamaratos, D. Vlachos, Y. Tomm, Chem. Phys. Letters **221**, 441 (1994).

[25] K. Wandelt, in *Physics and chemistry of alkali metal adsorption*, edited by H.P. Bonzel, A.M. Bradshaw, and G. Ertl (Elsevier, Amsterdam, 1989)

[26] C. Stampfl and M. Scheffler, Surf. Rev. Lett. **2**, 317 (1995).

[27] C.A. Papageorgopoulos and J.M. Chen, Surf. Sci. **39**, 313 (1973).

[28] C.A. Papageorgopoulos and J.M. Chen, Surf. Sci. **52**, 40 (1975).

[29] *CRC Handbook of Chemistry and Physics*, 64th edition. CRC Press, Boca Raton, FL, 1983.

[30] M.M. Dacorogna and M.L. Cohen, Phys. Rev. B **34**, 4996 (1986).

[31] M. Scheffler and C. Stampfl, *Electronic Structure*, Vol. 2, *Handbook of Surface Science*, K. Horn, M. Scheffler, (Elsevier, Amsterdam, 1999)

[32] I. Langmuir, J. Am. Chem. Soc. **54**, 2798 (1932).

[33] R.W. Gurney, Phys. Rev. **47**, 479 (1935).

[34] A. Kiejna and R.M. Nieminen Phys. Rev. B **66**, 085407 (2002).

[35] R. Adelung, R. Kunz, F. Ernst, L. Kipp, M. Skibowski, in *Advances in Solid State Physics* ed. by B. Kramer (Springer, Heidelberg, 2003) **43**, 463

[36] *Advanced Lithium Batteries*, eds O. Yamamoto and M. Wakihara, (Kodansha Press, 1998)

[37] W.Y. Liang, *Intercalation in Layered Materials*, edited by M.S. Dresselhaus (New York: Plenum 1986) p 31.

[38] C. Umrigar, D.E. Ellis, Ding-Sheng Wang, H. Krakauer, and M. Posternak, Phys. Rev. B **26**, 4935 (1982).

[39] H.E. Brauer, H.I. Starnberg, H.P. Hughes, L.J. Holleboom, Surf. Sci. **357-358**, 345 (1996).

[40] R.H. Friend and A.D. Yoffe, Adv. Phys. **36**, 1 (1987).

[41] T. Butz, A. Vasquez, H. Saitovitch, R. Mühlberger and A. Lerf, Physica B and C **99**, 69 (1980).

[42] J.E. Fischer and H.J. Kim, Phys. Rev. B **35**, 3295 (1987).

[43] T. Hibma, Physica B **99**, 136 (1980).

[44] A. Schellenberger, R. Schlaf, C. Pettenkofer, and W. Jaegermann, Phys. Rev. B **45**, 3538 (1992).

[45] H.E. Brauer, I. Ekvall, H. Olin, H.I. Starnberg, E. Wahlström, H.P. Hughes, and V.N. Strocov, Phys. Rev. B **55**, 10022 (1997).

[46] H.E. Brauer, H.I. Starnberg, L.J. Holleboom, V.N. Strocov, and H.P. Hughes, Phys. Rev. B **58**, 10031 (1998).

[47] C. Pettenkofer and W. Jaegermann, Phys. Rev. B **50**, 8816 (1994).

[48] M. Bronold, C. Pettenkofer, and W. Jaegermann, Appl. Phys. A **52**, 171 (1991).

[49] A. Schellenberger, PhD. Thesis, Freie Universität, Berlin (1992).

[50] M. Boehme, PhD. Thesis, Christian-Albrechts-Universität, Kiel (1998).

[51] D. Tonti, PhD. Thesis, Freie Universität, Berlin (2000).

[52] H.H. Weitering, J. Phys.: Condens. Matter **3**, 8535 (1991).

FIGURES

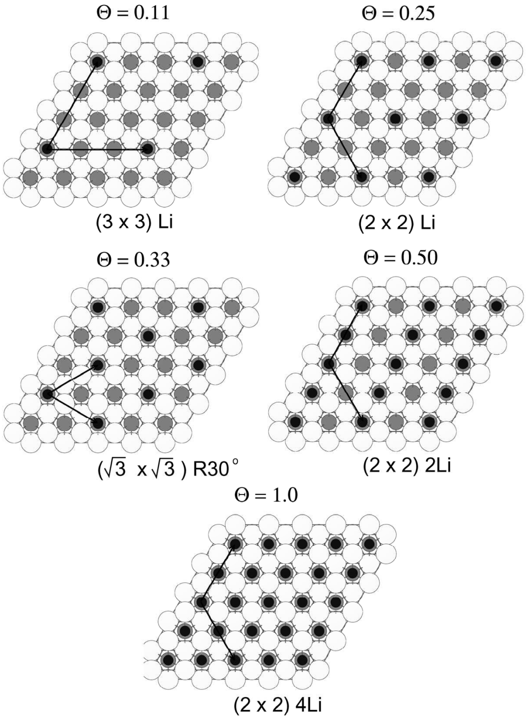

FIG. 1: Investigated supercells. Se (open circles), Ti (grey), and Li (dark grey with smaller radius).

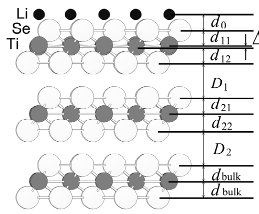

FIG. 2: Structure model of the geometrical changes induced by Li adsorption on $TiSe_2$ (0001), (referred to Table V).

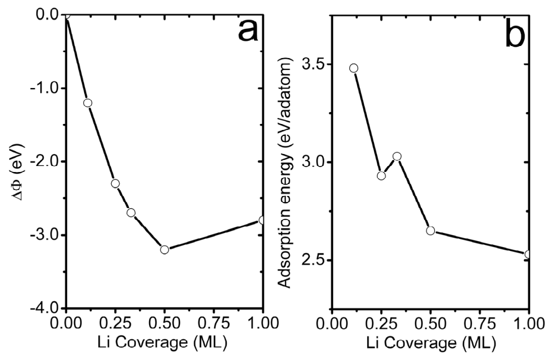

FIG. 3: Change of work function and adsorption energy with Li adsorbed on $TiSe_2$ at hcp sites.

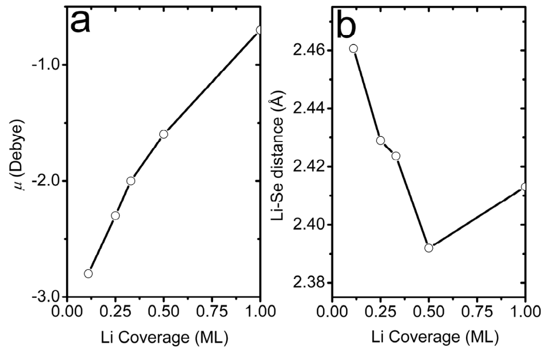

FIG. 4: Change of surface dipole moment and Li-Se distance for Li adsorbed on $TiSe_2$ at hcp sites.

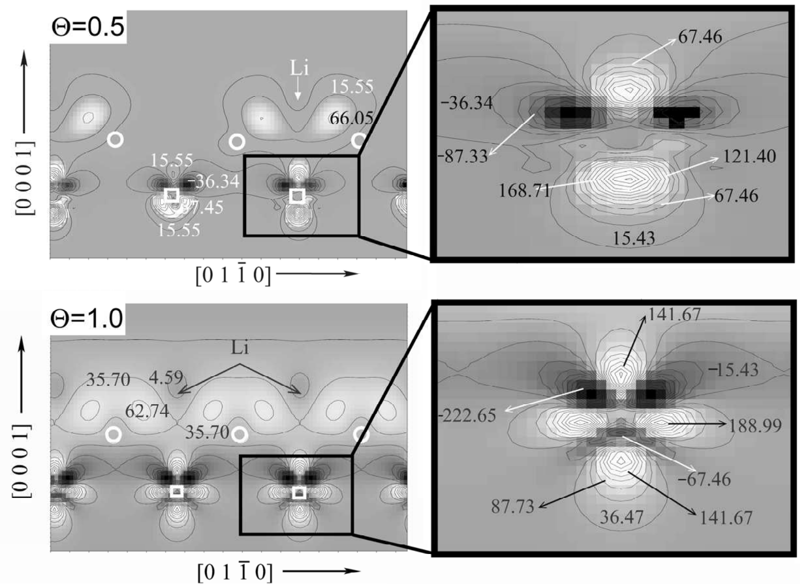

FIG. 5: Charge density difference, $n^{\Delta}(\mathbf{r})$, of Li adsorbed on $TiSe_2$ system, with $\Theta = 0.5$ and 1.0 for Li in the hcp site. n^{Li} is taken from a free, neutral atom; an enlarged picture of the frame in the left figure is given on its right. Circles indicate projected position of Se atoms in first atomic plane, and square Ti atoms. Arrows in left figure indicate the position of Li adatoms; contours are displayed in a plane perpendicular to the (0001) surface; units are 10^{-3} Å^{-3}.

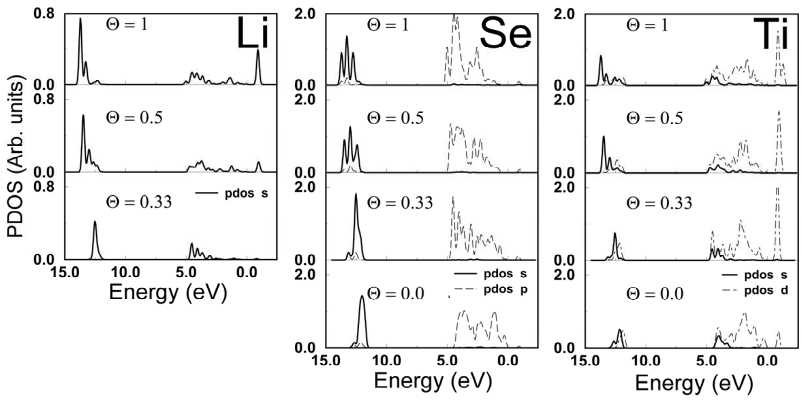

FIG. 6: PDOS for the Li-$TiSe_2$ (0001) system with Li adsorbed at the hcp sites. Partial density of states (PDOS) is decomposed in s, p, d components for Li, Se, and Ti.

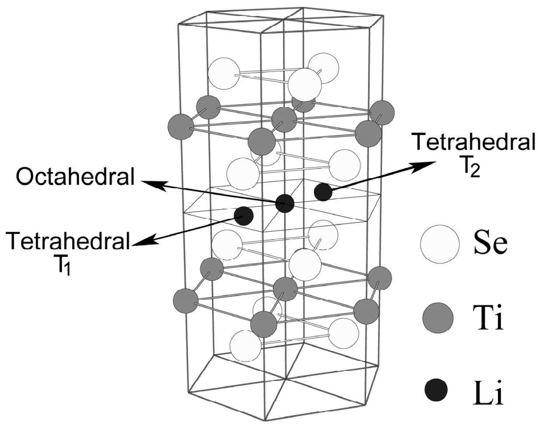

FIG. 7: Structure model of $TiSe_2$, showing occupation sites in van der Waals gap. Black Li spheres show three inter-sandwich sites, (one octahedral and two tetrahedral, T_1 and T_2).

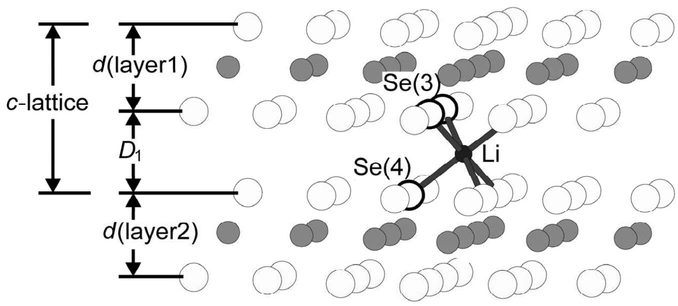

FIG. 8: Geometric structure of Li_xTiSe_2, showing Li in octahedral position and Se neighbors along its diffusion path across bridge to tetrahedral position.

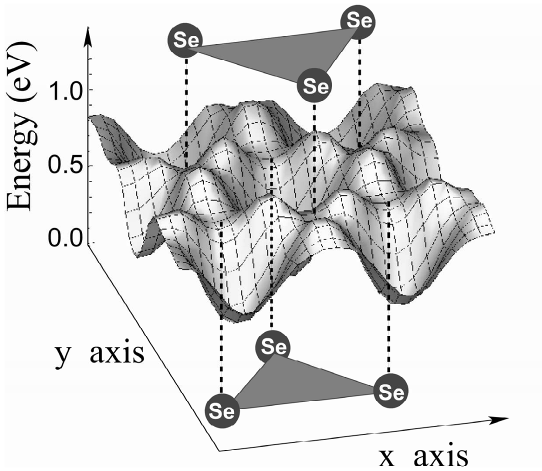

FIG. 9: Total energy of Li diffusion within van der Waals gap of bulk $TiSe_2$.

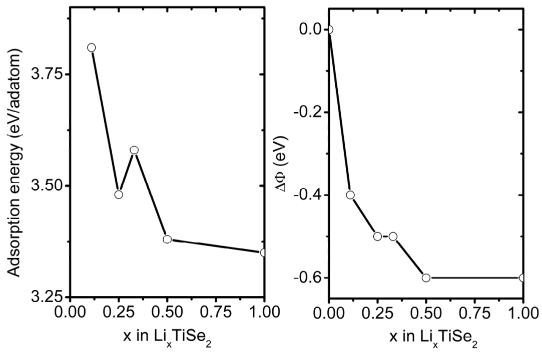

FIG. 10: Adsorption energy per Li atom and change of work function with Li in octahedral (van der Waals) sites.

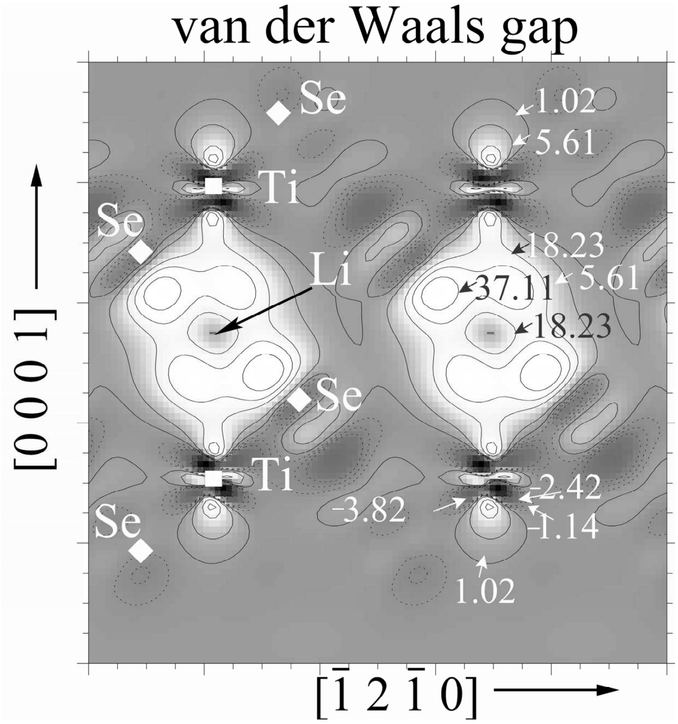

FIG. 11: Contour plot of electron difference density for Li at octahedral site localized in van der Waals gap. Contour units are 10^{-3} Å $^{-3}$.

TABLES

Coverage	d_0	d_{11}	d_{12}	Δd	D_1	d_{21}	d_{22}	D_2
				Li adsorbed on $TiSe_2$ (0001)				
0.00	-	1.50	1.50	0.00	3.26	1.51	1.51	3.21
0.11	1.37	1.59	1.44	-0.06	3.04	1.52	1.51	3.20
0.25	1.31	1.57	1.43	-0.03	3.17	1.51	1.52	3.08
0.33	1.31	1.56	1.47	-0.02	3.21	1.50	1.50	3.23
0.50	1.25	1.58	1.48	-0.02	3.12	1.51	1.52	3.10
1.00	1.32	1.63	1.46	0.00	3.14	1.51	1.52	3.07
		1rst (Se)	2nd (Ti)	3rd (Se)	4th (Se)	5th (Ti)	6th (Se)	
0.11		-0.20	-0.28	-0.21	0.00	0.00	0.00	
0.25		-0.24	-0.30	-0.22	-0.13	-0.13	-0.12	
0.33		-0.05	-0.11	-0.08	0.01	0.01	0.01	
0.50		-0.20	-0.28	-0.25	-0.11	-0.11	-0.11	

1.00	-0.18	-0.30	-0.25	-0.13	-0.13	-0.13

TABLE I: Calculated structural parameters (in Å) for Li at the $TiSe_2$ (0001) surface, with different coverages (upper block). Symbols are referred to Figure V. Shift in z-coordinate of atomic planes relativ to clean $TiSe_2$ surface system (bottom block); negative sign indicates a downward shift. Values for bare surface are averages over all three surface unit cells with variance in second decimal.

				Li_xTiSe_2				
x		d(layer1)	d(layer2)	D_1	d_zLiSe(3)	d_zLiSe(4)	dLiSe(3)	dLiSe(4)
0.11		3.03	3.04	3.15	1.60	1.60	2.59	2.59
0.25		3.02	3.00	3.22	1.61	1.62	2.59	2.60
0.33	octa	2.99	3.00	3.29	1.65	1.63	2.61	2.60
	bridge	3.01	3.02	3.28	1.92	1.51	2.21	2.34
	tetra	3.01	2.99	3.37	2.34	1.14	2.34	2.38
0.50		3.00	3.02	3.33	1.66	1.67	2.61	2.62
1.00		3.03	3.04	3.44	1.69	1.75	2.63	2.63

TABLE II: Structural parameters (in Å) for Li_xTiSe_2, with $0.11 \leq x \leq 1.0$, Li in the octahedral sites (for $x = 0.33$, also in bridge and tetrahedral T_1 sites are given). These data refer to Figure V. The distance d between atoms and the component in the z-direction d_z are also given.